The Astrophysical Journal, 700:937–944, 2009 August 1 doi:10.1088/0004-637X/700/2/937

THE RISE AND FALL OF OPEN SOLAR FLUX DURING THE CURRENT GRAND SOLAR MAXIMUM

M. Lockwood[1,2,3], A. P. Rouillard[1,2], and I. D. Finch[2]
[1] Space Environment Physics, School of Physics and Astronomy, Southampton University, Highfield, Southampton SO17 1BJ, UK; mike.lockwood@stfc.ac.uk
[2] Space Science and Technology Department, Rutherford Appleton Laboratory, Chilton, Didcot, Oxfordshire OX11 0QX, UK
Received 2009 April 3; accepted 2009 May 21; published 2009 July 7

ABSTRACT

We use geomagnetic activity data to study the rise and fall over the past century of the solar wind flow speed V_{SW}, the interplanetary magnetic field strength B, and the open solar flux F_S. Our estimates include allowance for the kinematic effect of longitudinal structure in the solar wind flow speed. As well as solar cycle variations, all three parameters show a long-term rise during the first half of the 20th century followed by peaks around 1955 and 1986 and then a recent decline. Cosmogenic isotope data reveal that this constitutes a grand maximum of solar activity which began in 1920, using the definition that such grand maxima are when 25-year averages of the heliospheric modulation potential exceeds 600 MV. Extrapolating the linear declines seen in all three parameters since 1985, yields predictions that the grand maximum will end in the years 2013, 2014, or 2027 using V_{SW}, F_S, or B, respectively. These estimates are consistent with predictions based on the probability distribution of the durations of past grand solar maxima seen in cosmogenic isotope data. The data contradict any suggestions of a floor to the open solar flux: we show that the solar minimum open solar flux, kinematically corrected to allow for the excess flux effect, has halved over the past two solar cycles.

Key words: interplanetary medium – solar–terrestrial relations – solar wind – Sun: magnetic fields

1. INTRODUCTION

Analysis of cosmogenic isotope abundances in terrestrial reservoirs, after removal of complicating factors such as the variability of the shielding afforded by the geomagnetic field, reveals the effect of the Sun in reducing the fluxes of galactic cosmic rays (GCRs) reaching the Earth. Because this solar shielding is known to vary with the strength and structure of the heliospheric magnetic field, both of which are modulated on both decadal and centennial timescales by solar activity, cosmogenic isotopes give us a unique insight into solar variability on millennial timescales. Such analyses indicate that the Sun has been unusually active over recent decades (Solanki et al. 2004; Vonmoos et al. 2006; Muscheler et al. 2007; Steinhilber et al. 2008). Solanki et al. (2004) used the ^{14}C isotope abundance found in tree trunks and concluded that the Sun has been more active recently than at any time in the previous 8000 years and that it was as active as in recent decades for only 10% of the past 11000 years. Vonmoos et al. (2006) employed ^{10}Be from the Greenland Ice core Project (GRIP) ice core in addition to ^{14}C. Their reconstruction is similar to that by Solanki et al., albeit not identical, but did not include the recent maximum as it ended at 390 years before the present day. Muscheler et al. (2007) also used both ^{10}Be and ^{14}C and their reconstruction is more significantly different to that of Solanki et al. in that, although recent activity was found to be high, it was not as exceptional, being at levels that were found for 20% of the time. Recently, Steinhilber et al. (2008) have made a composite of the above three reconstructions, also employing modern neutron monitor data and the Monte Carlo calculations of cosmogenic isotope production by Masarik & Beer (1999). These authors also ensured that inconsistencies between the reconstructions were eliminated: for example, a common interstellar GCR spectrum (the "Local Interstellar Spectrum" (LIS)) was adopted, which is assumed not to vary on the timescales considered. Figure 1 shows their results for 25-year means of the solar modulation potential ϕ which quantifies the GCR shielding effect of the heliosphere (Castagnoli & Lal 1980). Caballero-Lopez & Moraal (2004) have shown that ϕ is a good parameter for describing solar modulation at Earth of GCRs of energies above 0.1 GeV nucleon^{-1}, which covers the energy range of the GCRs responsible for the production of ^{10}Be in Earth's atmosphere (McCracken 2004). The peaks shaded black are where the 25-year averages of ϕ exceed the 600 MV level and include the recent high activity period (the average for 1954–2001 being 650 MV, shown by the arrow on the ϕ scale). These are grand maxima in solar activity. Note that the rise up to the current grand maximum in Figure 1 is very similar to that in heliospheric field strength B, as derived from ^{10}Be data for 1428 onward by McCracken (2007).

A key component of the GCR modulation quantified by ϕ is the open solar flux F_S, defined here to be the magnetic flux which enters the heliosphere by threading the coronal source surface (taken to be at heliocentric distance of $r = r_o = 2.5\ R_\odot = 2.5/215$ AU, where $R_\odot$ is the mean solar radius and AU is an astronomic unit). This results in a strong correlation between ϕ and F_S and hence strong anticorrelations between GCR fluxes at Earth and F_S (Lockwood 2001, 2003, 2006; Rouillard & Lockwood 2004; McCracken 2007). The open solar flux can be computed using the radial component of the interplanetary magnetic field (IMF), B_r, measured by a spacecraft (at a heliocentric distance r) because the *Ulysses* satellite has shown that the radial field is close to being independent of heliographic latitude λ (see the review by Lockwood & Owens 2009, and references therein). The signed (of one radial field polarity) open flux, F_S is therefore

$$F_S = 2\pi r^2 \langle |B_r|_T \rangle_{CR}. \quad (1)$$

The subscript CR denotes that the mean is taken over a full Carrington rotation in order to average out longitudinal structure; T is the timescale on which the B_r data are pre-averaged and then converted into absolute values. The value of T should be chosen so that it is not so large that the opposing

[3] Now at Department of Meteorology, University of Reading, Earley Gate, P.O. Box 243, Reading RG6 6BB, UK.

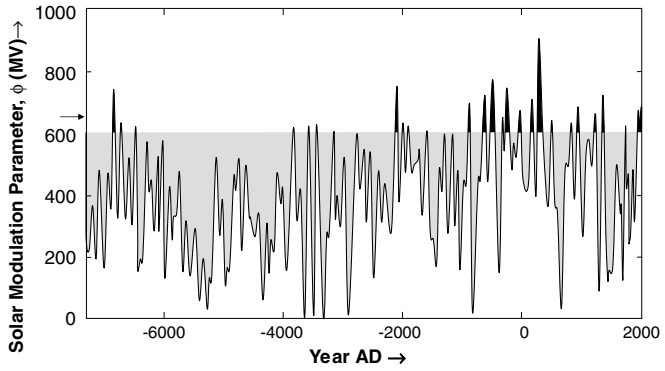

Figure 1. Composite variation of the solar modulation parameter, ϕ, derived from cosmogenic isotopes, with allowance for the geomagnetic field variation, by Steinhilber et al. (2008). The plot shows 25-year averages. The arrow gives the mean for 1954–2001 (650 MV). Intervals of high solar activity shaded black are defined by the $\phi = 600$ MV level.

field in Toward and Away interplanetary sectors of the field are cancelled (which would cause F_S to be underestimated) yet should be large enough to average out small-scale structure in the heliospheric field (which does not reflect structure in the source field and so would cause F_S to be overestimated; Wang & Sheeley 1995, 2002; Lockwood et al. 2006). Lockwood et al. (2004) used data from the first two perihelion passes of *Ulysses* to show that values of F_S derived using Equation (1) were accurate to within about 5% for averages over a full Carrington rotation (CR). Recently, Lockwood & Owens (2009) have used the survey of all data from spacecraft throughout the heliosphere by Owens et al. (2008) and at all phases of the solar cycle and have shown that CR averages of F_S obtained by Equation (1) are accurate to 2.5% for observations at $r < 2$ AU if the kinematic correction of Lockwood et al. (2009a) is applied first.

Lockwood et al. (1999) used this *Ulysses* result to reveal the centennial variation in open solar flux F_S for the first time. Their reconstruction was based on the aa geomagnetic index, which commences in 1868, and physical understanding of its relationship to interplanetary parameters. Various tests have indicated that there are some problems with the homogeneity of the calibration of the aa index, particularly after 1957 (Svalgaard & Cliver 2007a; Rouillard et al. 2007; Lockwood et al. 2009b). However, some of these tests have employed hourly average geomagnetic data which can have a significantly different dependence on interplanetary parameters to "range" geomagnetic indices such as aa (Rouillard et al. 2007; Svalgaard & Cliver 2007a; Lockwood et al. 2009b). Range indices are computed from the difference between maximum and minimum of H, the horizontal component of the field at Earth's surface, in 3 hr intervals: they have a strong dependence on solar wind speed V_{SW}, as well as on the IMF field strength, B. On the other hand, indices based on hourly means (usually of H) have only a weak dependence on V_{SW} and are largely controlled by B. The only exception to this is for magnetometer stations within the nightside auroral oval (i.e., under the electrojet of the substorm current wedge), hourly averages of the data from which show a strong $B(V_{SW})^2$ dependence (Finch et al. 2008). Hence, it is very important to avoid using most hourly mean geomagnetic data to either evaluate or correct aa. Lockwood et al. (2009b) show that most of the interval (1868–1968) compiled by the inventor of aa, Father Mayaud, it is remarkably accurate when tested using other range indices: however there are small calibration skips and drifts after 1957. Lockwood et al. (2009b) derived a corrected aa index, aa_C, using only the Ap (range) index and the k (range) indices derived by Clilverd et al. (2005) from the long sequences of Sodankylä and Niemegk magnetometer observations. Rouillard et al. (2007) used the aa_C index along with the annual index m, which is derived from the median standard deviation of hourly average geomagnetic data for each station-UT, as described by Lockwood et al. (2009b), to evaluate centennial variation in the solar wind speed, the IMF field magnitude and the open solar flux. These reconstructions extend back to only 1905 because before then the Niemegk magnetometer data comprise sampled "spot" values rather than full hourly means and the m index would be too heavily dependent on these data.

Some differences between the open solar flux reconstructions of Lockwood et al. (1999) and of Rouillard et al. (2007) arise from the corrections applied to aa to obtain aa_C, but the largest difference arises because the latter used an averaging timescale T of 1 day, whereas the former used $T = 1$ hr. The use of $T = 1$ day was adopted by Rouillard et al. because Lockwood et al. (2006) showed that it removes the "excess flux effect"—i.e., it makes the coronal source flux from near-Earth in situ observations approximately the same as that from solar magnetograph data, obtained using the potential field source surface (PFSS) method (Wang & Sheeley 1995, 2002).

Recently, Lockwood et al. (2009a) have shown that the difference between the open flux estimates from PFSS and from near-Earth observations (with $T = 1$ hr) is consistent with that found by Owens et al. (2008) elsewhere in the heliosphere. These authors also showed that this flux excess is well explained by the kinematic effects on the frozen-in interplanetary field of longitudinal structure in the solar wind flow speed on timescales of a solar rotation and less. Lockwood et al. (2009a) also derived a correction for this kinematic effect using the theory of Burlaga & Barouch (1976). The radial field at a given r is

$$B_r = (r_o/r)^2 B_{ro} + \Delta B_r, \tag{2}$$

where

$$\Delta B_r = [\partial V_{SW}/\partial t]_o \frac{(1 - r_o/r) B_{\phi r}}{\Omega V_{SW} \cos\lambda}. \tag{3}$$

B_{ro} is the radial component of the field at the coronal source surface $r = r_o$, λ is the heliographic latitude, Ω is the angular rotation velocity of the solar atmosphere, V_{SW} is the (radial) solar wind speed, $B_{\phi r}$ is the longitudinal field at r, and $[\partial V_{SW}/\partial t]_o$ is the temporal solar wind velocity gradient at $r = r_o$. The term $[\partial V_{SW}/\partial t]_o$ can be computed from solar wind measurements at r (which are intervals dt apart) by allowance for times of flight:

$$[\partial V_{SW}/\partial t]_o = dV_{SW}/[dt + \{(r - r_o)/V_{SW}\} - \{(r - r_o)/(V_{SW} + dV_{SW})\}]. \tag{4}$$

$B_{\phi r}$ is also measured and Ω and λ are known, hence the kinematic correction ΔB_r needed to obtain the source radial field B_{ro} from the value observed at r, B_r, can be computed from Equations (2)–(4) for each measurement of the solar wind and IMF. We here employ the procedure developed by Lockwood et al. (2009a) which smoothes the observed solar wind speed gradients with a 1-day time constant to account for the steepening effect in stream–stream interaction regions. Note that the equations of Burlaga & Barouch (1976) reduce to those of the Parker spiral in the limit $[\partial V_{SW}/\partial t]_o = 0$ (i.e., for longitudinally uniform solar wind flow).

In the present paper, we revisit the reconstructions of Rouillard et al. (2007) using the kinematic correction given by Equations (2)–(4). In addition, we employ an m index that has

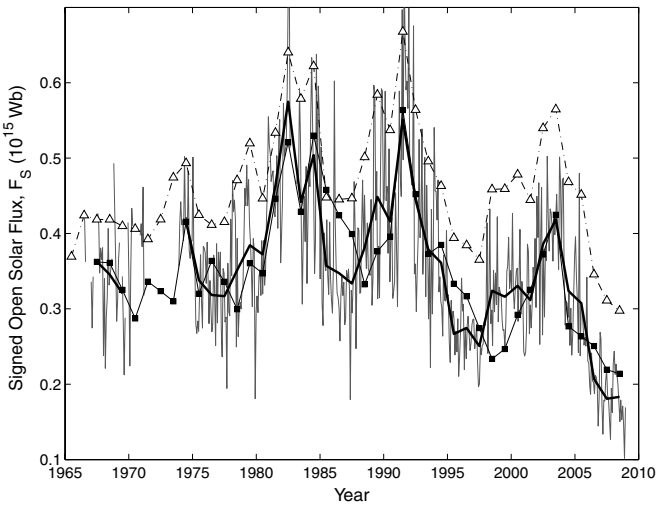

Figure 2. Various estimates of the signed open solar flux F_S. Dot-dashed line connecting open triangles: annual means of the signed flux threading the heliocentric sphere of radius $r = r_1 = 1$ AU, $2\pi {r_1}^2 |B_r|_{r\,=\,r1}$, derived from hourly means ($T = 1$ hr) of near-Earth in situ observations of the radial field. Thin dark gray line: CR averages of the signed flux threading the coronal source surface at $r = r_o = 2.5\ R_\odot = 2.5/215$ AU (where $R_\odot$ is the mean solar radius) derived from near-Earth interplanetary measurements by Lockwood et al. (2009a) using the kinematic correction to allow for the effect of longitudinal structure in the solar wind speed, $F_S = 2\pi {r_o}^2 |B_r|_{r\,=\,ro} = 2\pi {r_1}^2 (|B_r| - \Delta B_r)$. Solid black line: annual means of these kinematically corrected near-Earth measurements of F_S. Thin line connecting filled black squares: annual means of F_S derived from solar magnetograms using the PFSS method. Comparison of the dot-dashed line with the thick solid line reveals the flux excess for $r = r_1$.

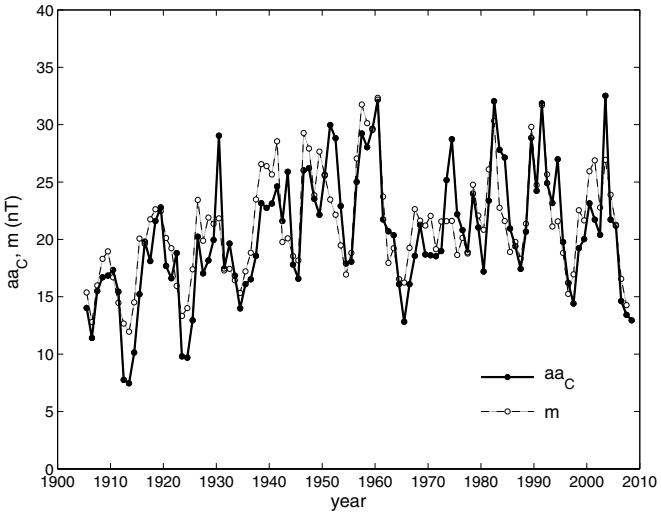

Figure 3. Geomagnetic activity indices employed in this paper. Thick black line connecting filled circles: annual means on the corrected aa index, aa_C, derived by Lockwood et al. (2009b) by correcting the standard aa index to allow for calibration jumps and drifts identified by comparison with other geomagnetic range data (and, crucially, without comparison to any index based on hourly average data). Dashed line connecting open circles: annual means of the median index m derived from the standard deviations of hourly mean geomagnetic data from a global network of stations by Lockwood et al. (2009b).

been improved with the addition of some additional data sequences from stations not previously available (Finch 2008).

In recent years, there have been indications that solar activity is declining again and that the current grand maximum is coming to an end. Lockwood (2003, 2004) noted that 11-year running means of the open solar flux had reached a peak in 1986 and that average GCR fluxes, as detected by ground-based neutron monitors, were subsequently increasing again. Lockwood & Fröhlich (2007) have shown that this decline in the average level of solar activity has continued (in sunspot numbers and total solar irradiance, as well as in open solar flux), as has the associated rise in cosmic-ray fluxes. Recently, Abreu et al. (2008) have used the distribution of durations of the grand solar maxima shown in Figure 1 (i.e., defined using cosmogenic isotope abundances) to estimate when the current grand maximum will end. Defining grand maxima with a threshold ϕ of 600 MV (in 25-year averages), as shown in Figure 1, the current one began in 1920 and the best estimate of its end date is 15 ± 8 years from the end of their data series (2004), i.e., between 2011 and 2027 (note that Abreu et al. actually employed a threshold ϕ of 616 MV to account for the effect of the high-pass data filter that they employed). In this paper, we study the centennial variations of solar wind speed V_{SW}, the IMF strength B, and the open solar flux F_S to test their consistency with this prediction.

2. INTERPLANETARY AND SOLAR CONDITIONS SINCE 1963

Since 1963, data on the solar wind and IMF have been available from spacecraft near Earth ($r \approx r_1 = 1$ AU). We here used the OMNI database of hourly means maintained by NASA's Space Physics Data Facility at Goddard Space Flight Center, in which the data have been lagged by the predicted propagation delay from the interplanetary monitor to the nose of Earth's magnetosphere. The thick black and the thin gray lines in Figure 2 show the open solar flux F_S derived by Lockwood et al. (2009a) using hourly means of the radial field magnitude ($T = 1$ hr), $|B_r|$, with the correction ΔB_r to allow for the kinematic effects associated with longitudinal structure in the solar wind speed, i.e., $F_S = 2\pi r_o^2 |B_r|_{r\,=\,ro} = 2\pi {r_1}^2 (|B_r| - \Delta B_r)$. The thin gray line shows the CR averages whereas the thick black line gives the annual means. These kinematically corrected open flux values can be compared with the thin line connecting filled black squares, which shows the annual means derived from solar magnetograms using the PFSS method (Wang & Sheeley 1995, 2002). In addition, the flux estimate without the kinematic correction, $2\pi {r_1}^2 |B_r|$ (with $T = 1$ hr) is given in Figure 2 by the dot-dashed line connecting open triangles. The difference between the dot-dashed line and the thick solid line is the "flux excess" at 1 AU. This has been successfully accounted for by the kinematic correction (a more physics-based method than the convenient use of $T = 1$ day).

Figure 3 shows the full sequences of annual means of the geomagnetic indices derived by Lockwood et al. (2009b) and used here, namely, the corrected aa index, aa_C (solid points), and the median index m (open circles), the latter derived from the standard deviations of hourly mean geomagnetic data from a global network of stations by treating each station-UT as a different data sequence. It can be seen that the two are similar but there are differences, both over recent solar cycles and in the long-term drift seen before 1950.

For the interval 1963–2008 these annual means have been correlated with annual means of $B(V_{SW})^n$, where B is the IMF field strength, V_{SW} is the solar wind speed, and n is an exponent that is here varied between -1 and $+3$ (note that hourly values of $B(V_{SW})^n$ are computed and then averaged into annual means). Finch & Lockwood (2007) analyzed the effect on such correlations of data gaps in the interplanetary observations and showed that the geomagnetic data should be masked so that data gaps are introduced to match those in the interplanetary

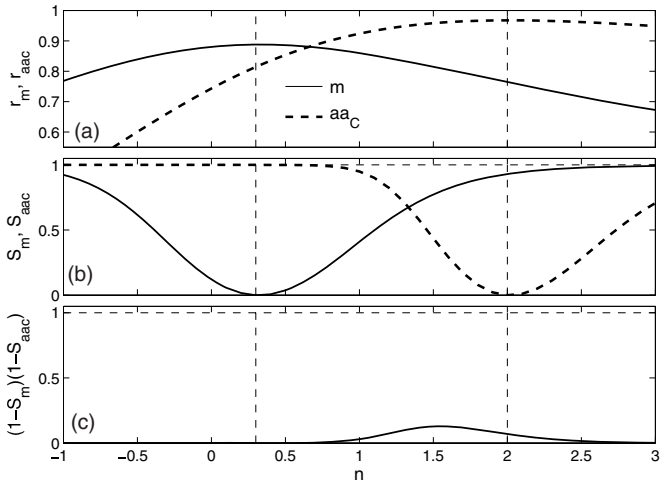

Figure 4. Analysis of the correlations between annual means of the aa_C (dashed line) and m (thin solid line) geomagnetic indices with the interplanetary parameter $B(V_{SW})^n$, where B is the IMF magnitude, V_{SW} is the solar wind speed, and the exponent n is varied between −1 and +3. (a) The correlation coefficients r_m and r_{aac} as a function of n. (b) The significances S_m and S_{aac} of the differences between the correlation coefficients at general n and their peak values. (c) The probability $(1 - S_m)(1 - S_{aac})$ that m and aa_C depend on the same $B(V_{SW})^n$ as a function of n.

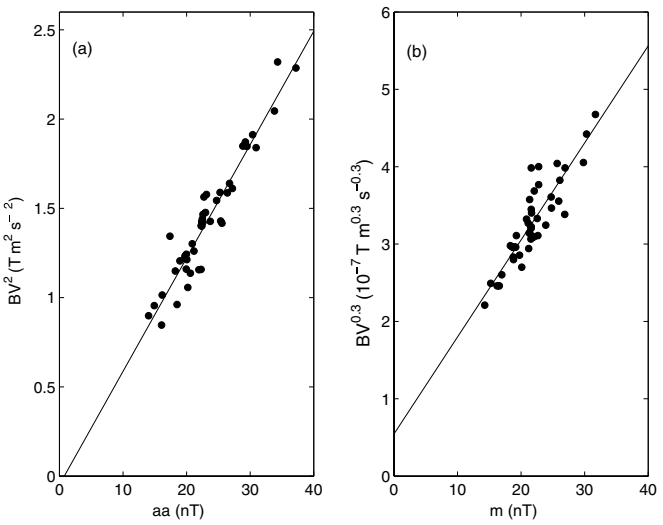

Figure 5. Scatter plots of annual mean data for the peak correlations shown in Figure 4(a). (a) aa_C against $B(V_{SW})^2$, (b) m against $B(V_{SW})^{0.3}$. The best-fit regression lines are derived using the Bayesian least-squares regression fit procedure described by Rouillard et al. (2007).

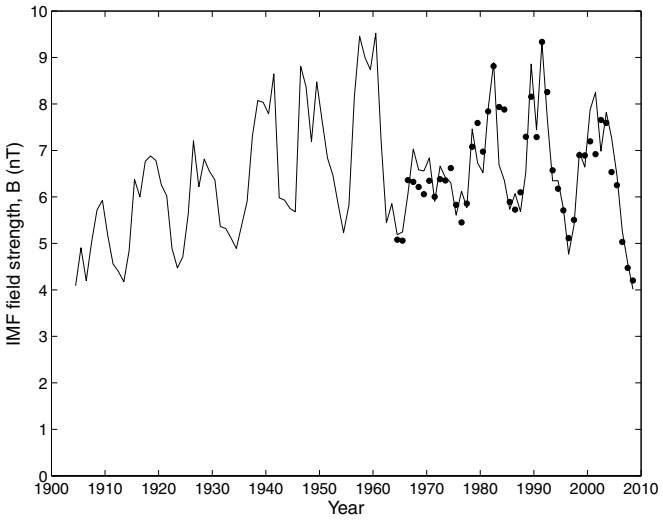

Figure 6. Extrapolated variation in IMF field strength B derived from the regression fits shown in Figure 5 (solid line) and the observed annual means from near-Earth measurements (filled circles).

data: hence the annual means include only simultaneous data (allowing for the propagation lag from the spacecraft to Earth's magnetosphere). This has been done here using the procedure described by Finch & Lockwood (2007).

The dashed line and thin solid lines in the top panel of Figure 4 show the correlation coefficients r_{aac} and r_m, respectively, between $B(V_{SW})^n$ and aa_C and between $B(V_{SW})^n$ and m, both as a function of n. The peak correlation for aa_C is $r_{aa} = 0.97$ for $n = 2$, the scatter plot for which is shown in Figure 5(a). Using the autoregressive AR-1 red noise model this correlation is significant at the $S_r > 99.999\%$ level. For this n, the correlation of $B(V_{SW})^2$ with m is $r_m = 0.75$ and using the Fisher's Z-test (of the significance of the difference between two correlation coefficients), we find this difference between r_{aa} and r_m for $n = 2$ is significant at the 99.98% level. The peak correlation for the median index m is $r_m = 0.89$ at $n = 0.3$ (with significance, evaluated against the AR-1 noise model of $S_r = 99.995\%$), the scatter plot for which is shown in Figure 5(b). At this n, the correlation with aa_C is $r_{aa} = 0.82$ and the significance of the difference between r_{aa} and r_m for $n = 0.3$ is 78.28%. The second panel of Figure 4 shows the significances S_m and S_{aac} of the differences between the correlation coefficients at general n and their peak values (at $n = 2$ for aa_C and at $n = 0.3$ for m). The bottom panel of Figure 4 shows, as a function of n, the probability $(1-S_m)(1-S_{aac})$ that m and aa_C depend on the same $B(V_{SW})^n$: it can be seen that the peak is at $n = 1.5$ but is only 0.13, which means that the difference in the dependence of m and aa_c on V_{SW} is significant at the 87% level.

The regression fits to the scatter plots in Figure 5 are generated using the Bayesian regression fit procedure described by Rouillard et al. (2007). Fits using ordinary least squares and median least squares procedures are almost identical because the scatter in the data is small.

3. INTERPLANETARY AND SOLAR CONDITIONS EXTRAPOLATED BACK TO 1905

We employ the regression fits shown in Figure 5 to extrapolate $B(V_{SW})^2$ and $B(V_{SW})^{0.3}$ back to 1905 from the geomagnetic data shown in Figure 3. From these we can compute the variations of B and V_{SW}. The results are shown in Figures 6 and 7. In both cases, the line gives the extrapolation based on the geomagnetic data and the filled circles give the annual means of the interplanetary observations.

The variation in the radial component of the IMF, B_r, and hence the open solar flux, F_S, has significant differences to the variation in B. This has two causes. First, for Parker spiral theory ($[\partial V_{SW}/\partial t]_o = 0$), the radial field is

$$|B_r|_{PS} = B \sin(\theta) = B/\{1 + [r_1\Omega/(V_{SW} \cos \lambda)]^2\}^{1/2}, \quad (5)$$

where the garden-hose angle θ is $\tan^{-1}\{V_{SW} \cos \lambda/(r_1\Omega)\}$. Thus, variations in the solar wind velocity V_{SW} introduce differences between the variations in B and in the open flux derived by assuming Parker spiral theory $[F_S]_{PS} = 2\pi r_1{}^2|B_r|_{PS}$ (Rouillard et al. 2007). However, this is not the only difference because Parker spiral theory is based on longitudinally uniform solar wind. Lockwood et al. (2009a) have shown that the observed

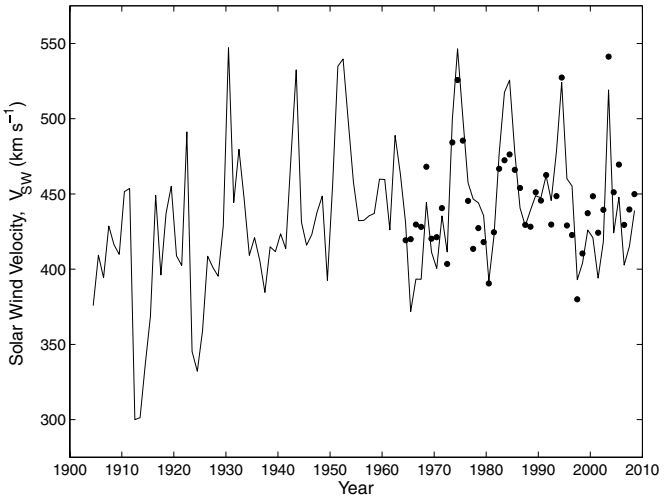

Figure 7. Same as Figure 6 for the solar wind speed, V_{SW}.

$|B_r|$ in the heliosphere, and hence F_S estimates by Equation (1), increase with r because of the kinematic effects of longitudinal structure in the solar wind (the "flux excess" effect). Thus, changes in both the mean solar wind velocity and its variability about the mean (on timescales < 27 days) decouple the B and F_S variations. Lockwood et al. (2009a) show that the observed radial field at $r_1 = 1$ AU, $|B_r|$, can be corrected by subtracting the kinematic correction, ΔB_r (Equation (2)) computed from the observed gradients in solar wind speed using Equations (3) and (4). The open flux $F_S = 2\pi r_o{}^2 |B_r|_{r\,=\,ro} = 2\pi r_1{}^2 (|B_r| - \Delta B_r)$ obtained this way is shown by the thin dark gray and thick black lines in Figure 2. Because annual means of both B and V_{SW} can be derived from the geomagnetic data (Figures 6 and 7), we can readily compute $|B_r|_{PS}$ and $[F_S]_{PS}$ by assuming Parker spiral theory (Equation (5)). Making the kinematic correction for historic data is not straightforward as we do not have a direct measure of the longitudinal structure in the solar wind velocity before the start of direct in situ observations in 1963. However, because the aa_C index has a dependence on the square of the solar wind velocity, the standard deviation of aa_C within a 27-day interval, σ_{aa}, is an approximate proxy for the kinematic correction (with the caveat that it also responds to changes in the magnitude and orientation of the IMF vector $\underline{\mathbf{B}}$ on short timescales). Figure 8 is a scatter plot of kinematically corrected radial field observed at $r_1 = 1$ AU, $(|B_r| - \Delta B_r)$, as a function of $(|B_r|_{PS} - [s\sigma_{aa} + c])$ where the value derived by assuming Parker spiral theory, $|B_r|_{PS}$ (see Equation (5)), is corrected using a linear function of σ_{aa}. It can be seen the scatter is reasonably small. The best-fit Bayesian regression gives $s = 0.060$ and $c = 0.916$. The correlation coefficient is 0.89, which evaluated against the AR-1 noise model, is significant at the 99.8% level.

Figure 9 shows the reconstructed open solar flux derived assuming Parker spiral theory, $[F_S]_{PS}$ (the dashed line with corresponding data points shown as open circles) and using the kinematic correction (black line and filled black circles).

3.1. Comparison of Open Solar Flux Reconstructions

Figure 10 compares the open solar flux reconstruction derived in the present paper with the prior ones by Rouillard et al. (2007) and Lockwood et al. (1999). In all three panels, the gray area bounded by thin lines gives annual means and the solid black lines show 11-year running means. All three reconstructions have been updated to the end of 2008. The

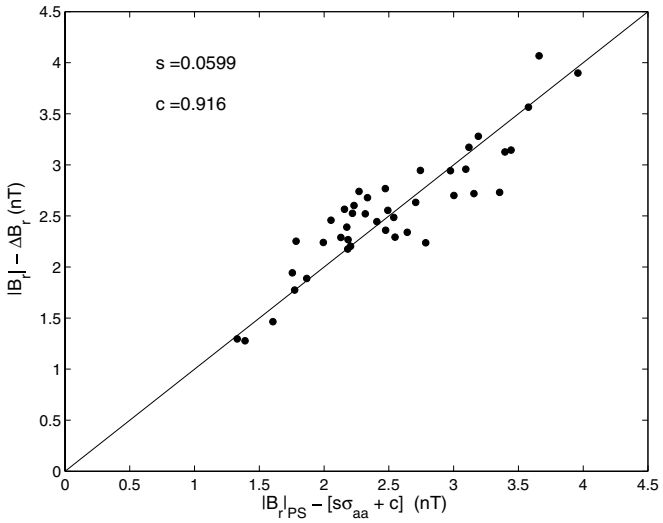

Figure 8. Scatter plot of kinematically corrected radial field observed at $r_1 = 1$ AU $(|B_r| - \Delta B_r)$, where $|B_r|$ is the absolute value of hourly means of the radial IMF component and ΔB_r is the kinematic correction factor for the "flux excess" effect due to longitudinal structure in the solar wind flow. Annual means are shown as a function of values derived assuming Parker spiral theory (for longitudinally constant solar wind flow) from observed B and V_{SW} values, $|B_r|_{PS}$. These Parker spiral values are corrected for the effect of longitudinal flow structure using the standard deviation of aa_C, σ_{aa}. The correlation coefficient is 0.89, which evaluated against the AR-1 noise model is significant at the 99.8% level.

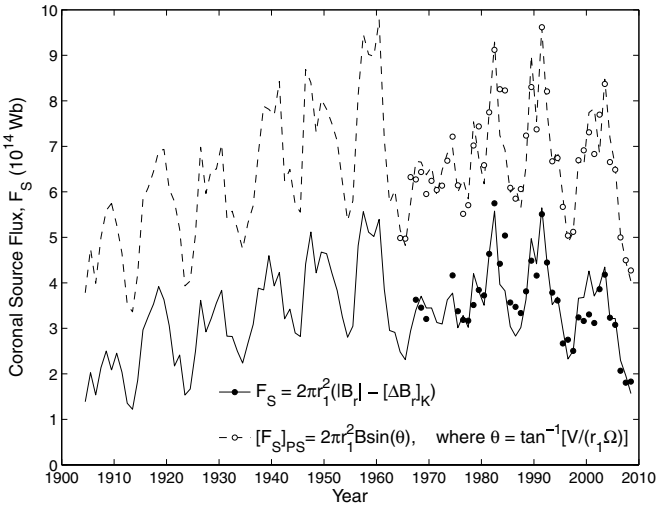

Figure 9. Same as Figure 6 for the open solar flux F_S. The dashed line and open circles show the results from the B and V_{SW} variations shown in Figures 6 and 7 by assuming Parker spiral theory. The black line and filled black circles show the results obtained using the kinematically corrected observed radial component of the IMF. The solid line has been derived from the value for Parker spiral theory using the regression fit shown in Figure 8.

differences in the derivations are that we have here used the kinematic correction to account for the flux excess effect (and so make the data consistent with PFSS estimates), whereas Rouillard et al. employed the averaging timescale of $T = 1$ day to make an allowance for the same effect and Lockwood et al. made no correction for the flux excess effect because they used $T = 1$ hr. In addition, we have here used a very slightly different m index which has been improved with data from a few more stations. Lockwood et al. used only the standard aa index, whereas this paper and that by Rouillard et al. employed the corrected aa index, aa_C. As a result of not allowing for the

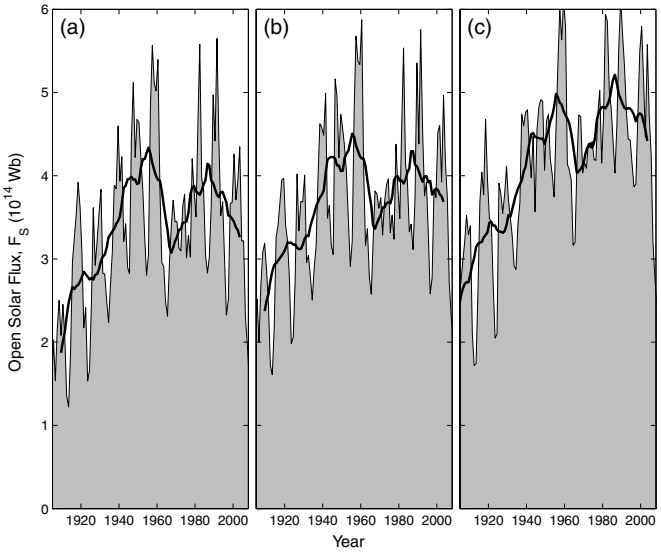

Figure 10. Comparison of reconstructions of the signed open solar flux F_S from geomagnetic activity data. Shaded gray areas bounded by the thin lines give annual means; the thick black lines give the 11-year running means. (a) The variation derived in Figure 9 of the present paper using hourly means ($T = 1$ hr) of radial IMF observations with the geomagnetic aa_C and m indices, and then corrected for the kinematic "excess flux" effect. (b) The variation derived from the aa_C and m indices by Rouillard et al. (2007) using and averaging timescale $T = 1$ day to account for the flux excess effect. (c) The variation derived by Lockwood et al. (1999) using $T = 1$ hr and the uncorrected aa index. The variation from Rouillard et al. is very close to that derived here. In (c), the effect of the calibration skip in aa around 1957 can be seen and all values are somewhat higher because the flux excess between the coronal source surface and 1 AU is not allowed for.

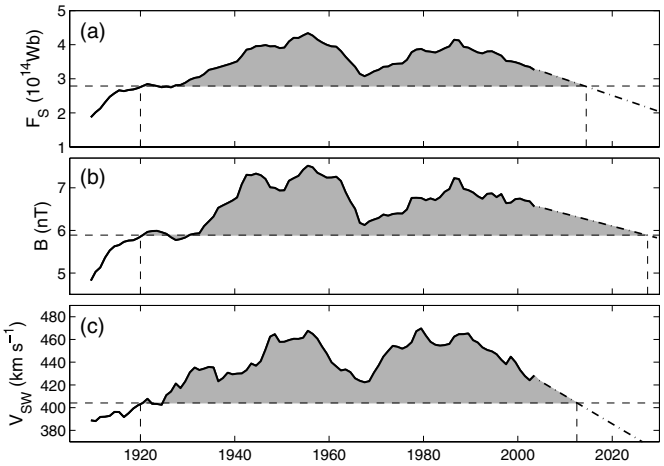

Figure 11. Prediction of the duration of the current grand maximum in solar activity. The solid lines give the 11-year running means of (from top to bottom) (a) the signed open flux F_S, (b) the IMF field strength B, and (c) the solar wind speed V_{SW} (as derived in Figures 8, 5, and 6, respectively). In each case, the horizontal dashed line marks the value in 1920, taken to be the onset of the current grand maximum in solar activity. The declines since 1986 are roughly linear in all three cases and are extrapolated forward in time by the linear fits shown by the dot-dashed lines. These extrapolations cross the 1920 level in 2014, 2027, and 2013 for F_S, B, and V_{SW}, respectively.

flux excess, the values in the Lockwood et al. reconstruction are consistently slightly higher than the other two. Inspection of Figure 10 shows that the use of $T = 1$ day by Rouillard et al. gave results very similar indeed to the kinematic correction employed here, although values before about 1940 are slightly lower in Figure 10(a) than in Figure 10(b), as they are for after 1990 (in both the fitted reconstruction and the interplanetary data). The second major difference of the Lockwood et al. reconstruction (Figure 10(c)) is that the 1985 peak is larger than that in 1955, whereas it is slightly lower in the other two reconstructions. Lockwood et al. (2009b) show that this arises from the calibration glitch in the original aa data in 1957 (when the northern hemisphere site moved from Abinger to Hartland) which has been compounded by slow subsequent drifts in the same sense in both the northern and southern hemisphere data. It is interesting to note that Figures 10(a) and (b) are more consistent with the reconstruction of open flux from ^{10}Be abundances by McCracken (2007) in which these two peaks are of roughly equal magnitude. In the reconstruction by Lockwood et al. (1999) the peak of the smoothed (11-year running mean) variation in 1955 is 83% larger than the value for 1910 whereas the 1986 peak was 93% higher. In the reconstruction by Rouillard et al., these values are slightly lower (89% and 81%, respectively) and in the kinematically corrected reconstruction presented here they are 132% and 121%.

3.2. The Progress of the Current Grand Maximum

Figure 11 shows the variations of the 11-year running means of (a) the open solar flux, F_S; (b) the IMF field strength, B; and (c) the solar wind speed V_{SW}. The area shaded gray is where each exceeds its value in 1920, which is the onset of the current grand maximum, as defined by 25-year means of ϕ and the 600 MV threshold in Figure 1. The data available extend up to the end of 2008 and so 11-year running means are available to the middle of 2002. The dashed lines bounding the gray areas in Figure 11 after this date are linear extrapolations based on a fit to the 11-year running means between 1986 and 2002.

It can be seen that all three parameters show similar variations during the grand maximum with two peaks separated by a relative minimum around 1968. If the linear extrapolations are used to predict the end of the grand maximum (by where they cross their respective 1920 levels), this occurs in 2014, 2027, and 2013 for F_S, B, and V_{SW}, respectively. The likely validity of these simple extrapolations is discussed in the next section.

4. CONCLUSIONS

We have employed the kinematic correction to observed radial fields at 1 AU to allow for the flux excess effect on open flux estimates from in situ spacecraft data (Owens et al. 2008; Lockwood et al. 2009a). The results are very similar to those of Rouillard et al. (2007) who employed averaging (over $T =$ 1 day) to allow for this effect and make the in situ data consistent with the estimates obtained from solar magnetograms using the PFSS method (Wang & Sheeley 1995, 2002). However, the results are not identical and the kinematic correction gives a slightly greater upward trend in open solar flux in the first half of the 20th century and a slightly faster decline since the peak in 1986.

Svalgaard & Cliver (2007b) propose that there is a minimum "floor" value to the IMF strength B of 4.6 nT in annual mean data and a minimum to the open solar flux of 4×10^{14} Wb. We note that the observed annual mean of B for 2008 has already fallen to 4.2 nT in the current solar minimum, but we do here find that the value of B has indeed been above 4 nT at all times since 1905. McCracken (2007) proposes that the concept of floors in B may indeed be valid, but notes that since 1428 there must have been at least four upward steps in such a floor to reach present-day values, the floor value for 1428–1528 being

less than a 10th of today's value. If the minimum B does change in discrete steps, as opposed to continuously, the reasons for this are not yet understood.

Svalgaard & Cliver's estimate of a "floor" open flux comes from the observed radial field during the 1996 solar minimum only (without allowance for the flux excess effect) and they tacitly assume that, because B is near its apparent floor at this time, the open flux will also be near a minimum value. We here stress here the point made by Lockwood et al. (2006) and Rouillard et al. (2007) that the variation in open solar flux F_S is decoupled from that in the IMF magnitude B by variations in the solar wind speed (which winds/unwinds the Parker spiral) and, more importantly, by the kinematic effect of longitudinally structured solar wind flow (which causes additional radial field with increasing distance from the Sun: the excess flux effect). Neither of these effects is allowed for by Svalgaard & Cliver when they suggest that a floor in B would also imply a floor in the open solar flux of 4×10^{14} Wb.

Because they do not allow for the kinematic effect of longitudinal flow, Svalgaard & Cliver's open flux "floor" estimate is directly comparable to the dot-dashed line (joining open triangles) in Figure 2, which shows that annual means of $2\pi {r_1}^2 |B_r|_{r\,=\,r1}$, far from being constant, fell from 4.50×10^{14} Wb, to 3.65×10^{14} Wb, to 3.00×10^{14} Wb for 1985, 1997, and 2008, respectively (associated with the last three solar minima). Thus, the sunspot minimum flux threading the heliocentric sphere of radius $r_1 =$ 1 AU ($2\pi {r_1}^2 |B_r|_{r\,=\,r1}$) was 50% higher just two solar cycles ago than it was during the recent solar minimum. The kinematic correction for the flux excess effect means that the true open solar fluxes $F_S = 2\pi {r_o}^2 |B_r|_{r\,=\,ro} = 2\pi {r_1}^2 (|B_r| - \Delta B_r)_{r\,=\,r1}$ in these minima are lower than the above values (as shown by comparison of the solid and dot-dashed lines in Figure 2): the open solar flux for the above three years being 3.57×10^{14} Wb, 2.51×10^{14} Wb, and 1.80×10^{14}, respectively. Thus, the decline in the kinematically corrected open flux at sunspot minimum is so great that it was 98% higher just two cycles ago than during the recent minimum. The idea of a floor in the open solar flux is in direct contradiction with the in situ measurements.

Hence, direct in situ observations near Earth, with allowance for the flux excess effect (which causes the radial field increase with increasing heliocentric distance Owens et al., 2008; Lockwood et al., 2009a), show that for 2007 and 2008 the annual mean open solar flux fell to 1.8×10^{14} Wb (thick line Figure 2), and these years are still within the grand maximum of solar activity, as defined by the $\phi = 600$ MV level in 25-year means. Our reconstructed open solar flux is near 1.3×10^{14} Wb during the first solar minimum following the start of reliable hourly mean geomagnetic data in 1905. From the uncertainties in the regression fits we find that this value has an uncertainty of $\pm 0.2 \times 10^{14}$ Wb at the two sigma level, an error of $\pm 15\%$. The other uncertainty is the use of the *Ulysses* result of the latitudinal invariance of the radial field. This has been shown to introduce errors of, at most, $\pm 2.5\%$ for all observations inside $r = 2$ AU by Lockwood & Owens (2009) and so does not introduce as much uncertainty.

Figure 12 is a scatter plot of reconstructed open solar flux F_S as a function of reconstructed IMF strength, B for 1905–2008. The black line is a fourth-order polynomial fit, constrained to pass though the origin. This constraint is applied because if the coronal source flux could fall to zero, then the IMF near Earth would certainly also fall to zero. The gray area bounded by dashed lines gives the uncertainty in the fitted polynomial. The reconstructions for 1905 onward do not vary greatly from

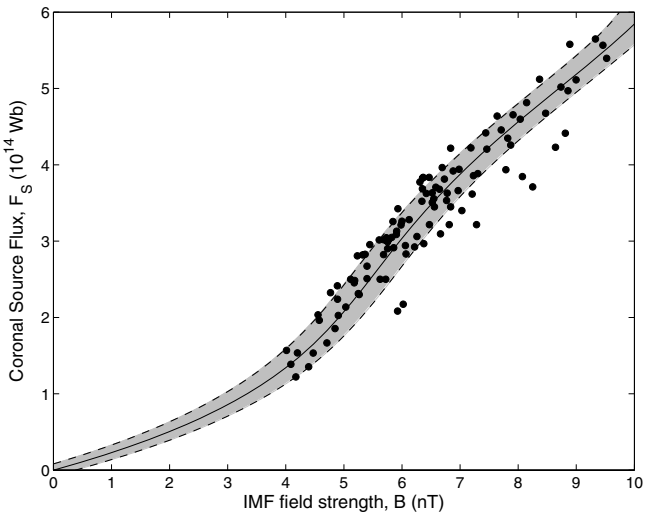

Figure 12. Scatter plot of reconstructed open solar flux F_S as a function of reconstructed IMF strength, B for 1905–2008. The black line is a fourth-order polynomial fit, constrained to pass though the origin. The gray area bounded by dashed lines is plus and minus the fit error around this best-fit line.

a linear variation, but Figure 12 gives evidence that there are two competing effects which cause a deviation from a linear variation. The first is what would be seen for uniform solar wind flow (over a 27-day period), as predicted by Parker spiral theory. As the average B rises we here find the average solar wind speed V_{SW} also rises (see Figures 6 and 7). This causes the spiral field to unwind and the ratio ($|B_r|/B$) rises, and hence the ratio (F_S/B) also rises as B rises. This is consistent in sense with the non-linear behavior seen at B below about 6 nT (and for the constrained polynomial fit). However, at B above about 6 nT, the ratio (F_S/B) falls as B continues to increase. This is consistent with an increased kinematic effect due to increased longitudinal structure in the solar wind at higher solar activity which will increase the B at 1 AU for a given F_S. The data points are mainly from within the current grand solar maximum defined by $\phi = 600$ MV in 25-year means (only those for 1905–1920 are not) and all are within a period for which these means of ϕ exceed 575 MV. Figure 1 shows many intervals when 25-year means of ϕ fall to near zero (grand solar minima, when the cosmic-ray spectrum reaching Earth approached the LIS) and hence there is certainly no evidence for an absolute "floor" in the heliospheric field in cosmogenic isotope data as suggested by Svalgaard & Cliver (2007b): indeed, these data suggest that the heliospheric field can fall considerably below the values seen during the space age which is within a grand solar maximum. Hence, as pointed out by McCracken (2007), if floors in B do exist they generally last for of order 100 years and successive jumps between floors must have brought about a net increase by a factor of 10 over the past 600 years. We also note that a floor in the IMF B at 1 AU would not imply a floor in the open solar flux because the variations in the two are decoupled by any variations in the average speed of the solar wind and the kinematic flux excess effect of its longitudinal flow structure. From the analyses of cosmogenic isotopes (e.g., McCracken 2007; Solanki et al. 2004; Vonmoos et al. 2006; Muscheler et al. 2007; Steinhilber et al. 2008) it is to be expected that data points from grand solar minima would appear in the gray shaded area at $B < 4$ nT and $F_S < 1 \times 10^{14}$ Wb in Figure 12.

Figure 11 shows that the signed open flux F_S, the IMF field strength B, and the solar wind speed V_{SW} have all had simi-

lar long-term temporal variations during the current grand solar maximum. All three have shown an almost linear decline since 1986. Of course, this decline need not remain linear and may even be interrupted by another rise before the present grand solar maximum finally ends. However, Figure 11 shows that the running means by the end of the sequences have reached values not much greater than the thresholds which would mark the end of the grand maximum (as defined by 25-year means of ϕ and the 600 MV level) and so the linear extrapolation of these declines are likely to yield reasonably valid predictions of the date at which the grand maximum will end. This occurs in 2014, 2027, or 2013 if we extrapolate using F_S, B, or V_{SW}, respectively. The best estimate would be a mean of these, weighted by their contributions to ϕ: quantifying those weighting factors will be the subject of a further study. However, we can compare these dates with the prediction by Abreu et al. (2008), based on the probability distribution of the durations of grand maxima in the solar modulation potential variation derived from cosmogenic isotopes. These authors found the statistics were best described by a gamma probability distribution function, for which (at the 2σ uncertainty level) the grand maximum will end 15 ± 8 years after 2004, i.e., in the interval 2011–2027, but the authors note that early dates in this range are more likely than later ones. Thus, the behavior and trends identified here give strong support to the prediction of Abreu et al. (2008).

We thank Yi-Ming Wang for the provision of the PFSS data and Friedhelm Steinhilber, Jose Abreu, and Jürg Beer for many helpful discussions and the modulation potential data series. We are also grateful to the great many scientists who made possible the recording, storing, and distribution of both the interplanetary and geomagnetic activity data employed in this paper. The interplanetary data were supplied by the OMNI web pages of the Space Physics Data Facility at NASA/Goddard Space Flight Center and the magnetometer data were obtained from the World Data Centre network, the British Geological Survey, and Leif Svalgaard. This research was supported by the UK Science and Technology Facilities Council.

REFERENCES

Abreu, J. A., Beer, J., Steinhilber, F., Tobias, S. M., & Weiss, N. O. 2008, Geophys. Res. Lett., 35, L20109
Burlaga, L. F., & Barouch, E. 1976, ApJ, 203, 257
Caballero-Lopez, R. A., & Moraal, H. 2004, J. Geophys. Res., 109, A01101
Castagnoli, G., & Lal, D. 1980, Radiocarbon, 22, 133
Clilverd, M. A., Clarke, E., Ulich, T., Linthe, H. J., & Rishbeth, H. 2005, J. Geophys. Res., 110, A07205
Finch, I. D. 2008, PhD thesis, Univ. of Southampton
Finch, I. D., & Lockwood, M. 2007, Ann. Geophys., 25, 495
Finch, I. D., Lockwood, M., & Rouillard, A. P. 2008, Geophys. Res. Lett., 35, L21105
Lockwood, M. 2001, J. Geophys. Res., 106, 16021
Lockwood, M. 2003, J. Geophys. Res., 108, 1128
Lockwood, M. 2004, in the Saas-Fee Advanced Course 34, The Sun, Solar Analogs and the Climate, ed. I. Rüedi, M. Güdel, & W. Schmutz (Berlin: Springer), 107
Lockwood, M. 2006, Space Sci. Rev., 125, 95
Lockwood, M., Forsyth, R. B., Balogh, A., & McComas, D. J. 2004, Ann. Geophys, 22, 1395
Lockwood, M., & Fröhlich, C. 2007, Proc. R. Soc. A, 463, 2447
Lockwood, M., & Owens, M. 2009, ApJ, submitted
Lockwood, M., Owens, M., & Rouillard, A. P. 2009a, J. Geophys. Res., submitted
Lockwood, M., Rouillard, A. P., Finch, I. D., & Stamper, R. 2006, J. Geophys. Res., 111, A09109
Lockwood, M., Stamper, R., & Wild, M. N. 1999, Nature, 399, 437
Lockwood, M., et al. 2009b, Ann. Geophys., submitted
Masarik, J., & Beer, J. 1999, J. Geophys. Res., 104, 12099
McCracken, K. G. 2004, J. Geophys. Res., 109, A04101
McCracken, K. G. 2007, J. Geophys. Res., 112, A09106
Muscheler, R., Joos, F., Beer, J., Müller, S. A., Vonmoos, M., & Snowball, I. 2007, Quat. Sci. Rev., 26, 82
Owens, M. J., Arge, C. N., Crooker, N. U., Schwadron, N. A., & Horbury, T. S. 2008, J. Geophys. Res., 113, A12103
Rouillard, A. P., & Lockwood, M. 2004, Ann., Geophys., 22, 4381
Rouillard, A. P., Lockwood, M., & Finch, I. D. 2007, J. Geophys. Res., 112, A05103
Solanki, S. K., Usoskin, I. G., Kromer, B., Schüssler, M., & Beer, J. 2004, Nature, 431, 1084
Steinhilber, F., Abreu, J. A., & Beer, J. 2008, Astrophys. Space Sci. Trans., 4, 1
Svalgaard, L., & Cliver, E. W. 2007a, J. Geophys. Res., 112, A10111
Svalgaard, L., & Cliver, E. W. 2007b, ApJ., 661, L203
Vonmoos, M., Beer, J., & Muscheler, R. 2006, J. Geophys. Res., 111, A10105
Wang, Y.-M., & Sheeley, N. R., Jr. 1995, ApJ, 447, L143
Wang, Y.-M., & Sheeley, N. R., Jr. 2002, J. Geophys. Res., 107, 1302